

Children's Mercy Kansas City

SHARE @ Children's Mercy

Manuscripts, Articles, Book Chapters and Other Papers

4-2018

Short Term Development and Fate of MGE-Like Neural Progenitor Cells in Jaundiced and Non-Jaundiced Rat Brain.

Fu-Chen Yang

Julia Draper

Peter G Smith

Jay L. Vivian

Steven Shapiro

Children's Mercy Hospital

See next page for additional authors

Let us know how access to this publication benefits you

Follow this and additional works at: <https://scholarlyexchange.childrensmc.org/papers>



Part of the [Neurology Commons](#)

Recommended Citation

Yang FC, Draper J, Smith PG, Vivian JL, Shapiro SM, Stanford JA. Short Term Development and Fate of MGE-Like Neural Progenitor Cells in Jaundiced and Non-Jaundiced Rat Brain. *Cell Transplant*. 2018;27(4):654-665. doi:10.1177/0963689718766327

This Article is brought to you for free and open access by SHARE @ Children's Mercy. It has been accepted for inclusion in Manuscripts, Articles, Book Chapters and Other Papers by an authorized administrator of SHARE @ Children's Mercy. For more information, please contact hlsteel@cmh.edu.

Creator(s)

Fu-Chen Yang, Julia Draper, Peter G Smith, Jay L. Vivian, Steven Shapiro, and John A. Stanford

Short Term Development and Fate of MGE-Like Neural Progenitor Cells in Jaundiced and Non-Jaundiced Rat Brain

Cell Transplantation
2018, Vol. 27(4) 654–665
© The Author(s) 2018
Reprints and permission:
sagepub.com/journalsPermissions.nav
DOI: 10.1177/0963689718766327
journals.sagepub.com/home/cil


Fu-Chen Yang¹, Julia Draper², Peter G. Smith^{1,3}, Jay L. Vivian⁴, Steven M. Shapiro⁵, and John A. Stanford^{1,3}

Abstract

Neonatal hyperbilirubinemia targets specific brain regions and can lead to kernicterus. One of the most debilitating symptoms of kernicterus is dystonia, which results from bilirubin toxicity to the globus pallidus (GP). Stem cell transplantation into the GP to replace lost neurons and restore basal ganglia circuits function is a potential therapeutic strategy to treat dystonia in kernicterus. In this study we transplanted human medial ganglionic eminence (MGE)-like neural progenitor cells (NPCs) that we differentiated into a primarily gamma-aminobutyric acid (GABA)ergic phenotype, into the GP of non-immunosuppressed jaundiced (jj) and non-jaundiced (Nj) rats. We assessed the survival and development of graft cells at three time-points post-transplantation. While grafted MGE-like NPCs survived and generated abundant fibers in both jj and Nj brains, NPC survival was greater in the jj brain. These results were consistent with our previous finding that excitatory spinal interneuron-like NPCs exhibited a higher survival rate in the jj brain than in the Nj brain. Our findings further support our hypothesis that slightly elevated bilirubin levels in the jj brain served as an antioxidant and immunosuppressant to protect the transplanted cells. We also identified graft fibers growing toward brain regions that receive projections from the GP, as well as host fibers extending toward the graft. These promising findings suggest that MGE-like NPCs may have the capacity to restore the circuits connecting GP and other nuclei.

Keywords

Bilirubin encephalopathy, globus pallidus, Gunn rat, xenotransplantation, MGE-like NPC, immunosuppressant

Introduction

Neonatal jaundice due to elevated blood bilirubin levels occurs in up to 85% of newborns¹. When bilirubin levels exceed the binding capacity of albumin, excess free unconjugated bilirubin enters the brain where it targets specific nuclei, including the globus pallidus (GP), subthalamic nucleus, inferior colliculus, hippocampus, and cerebellum^{2,3}. Free bilirubin is toxic and can lead to kernicterus, which is a devastating and permanent neurological syndrome. Currently, there is no effective cure for kernicterus. Because it strikes during infancy, affected individuals and their families are subjected to a lifetime of dependency on caregivers.

Among the most debilitating symptoms of kernicterus is painful dystonia resulting from damage to the GP². The GP is a key relay nucleus in the basal ganglia pathway. Due to the toxic effects of bilirubin in the GP, we believe that targeting this nucleus with neuronal stem cells to replace the lost neurons and reconstruct basal ganglia circuit function is a logical therapeutic approach for treating dystonia in

¹ Department of Molecular & Integrative Physiology, University of Kansas Medical Center, Kansas City, KS, USA

² Transgenic and Gene Targeting Institutional Facility, University of Kansas Medical Center, Kansas City, KS, USA

³ Kansas Intellectual & Developmental Disabilities Research Center, University of Kansas Medical Center, Kansas City, KS, USA

⁴ Department of Pathology & Laboratory Medicine, University of Kansas Medical Center, Kansas City, KS, USA

⁵ Division of Child Neurology, Department of Pediatrics, Children's Mercy Hospital & Clinics, Kansas City, MO, USA

Submitted: October 2, 2017. Revised: February 5, 2018. Accepted: February 19, 2018.

Corresponding Author:

John A. Stanford, Department of Molecular & Integrative Physiology, University of Kansas Medical Center, 3901 Rainbow Blvd., MS 3051, Kansas City, KS 66160, USA.
Email: jstanford@kumc.edu



kernicterus. Research into neonatal jaundice and kernicterus has been facilitated by the use of the Gunn rat model⁴. Homozygous jaundiced Gunn rats (jj) rats lack the gene for uridine diphosphate glucuronosyl transferase, the enzyme responsible for bilirubin conjugation and elimination. This leads to hyperbilirubinemia⁵. Using this model, we recently reported that excitatory spinal cord interneuron-like neural progenitor cells (NPCs) had a greater survival rate in the jj brain than in the non-jaundiced (Nj) brain⁶.

The goal of the current study was to develop and test more GP-like NPCs in the Gunn rat model. With the exception of ~5% that are cholinergic, most of the neurons in the GP are gamma-aminobutyric acid (GABA)ergic. Among these GABAergic neurons, at least 50–60% co-express parvalbumin (PV)^{7–9}, while a smaller population expresses preproenkephalin (PPE)⁸. There are multiple embryological origins of GP neurons. Most (~70%) are derived from the caudoventral portion of the medial ganglionic eminence (MGE), while the lateral ganglionic eminence generates about 25% and the preoptic area gives rise to the other 5%⁹. We chose NPCs derived from the WA09 human embryonic stem cell line (hESC) and differentiated into MGE-like NPCs. Upon differentiation, these cells phenotypically resemble GABAergic neurons in the basal ganglia. These cells were transplanted into the GP of jj Gunn rats and their non-jaundiced (Nj) littermates, and assessed for graft survival and development.

Materials and Methods

Propagation and Preparation of Human NPCs for Transplantation

Pluripotent stem cell culture. WA09 human embryonic stem cells¹⁰ were maintained in an undifferentiated state by culture on Matrigel in mTeSR media (Corning 354277, Corning, Tewksbury, MA, USA). Cells were passaged every 4 days with ReLeSR reagent (Stem Cell Technologies 05872, Stem Cell Technologies, Vancouver, BC, Canada).

Pluripotent stem cell aggregation and differentiation. Embryoid body (EB) formation and culture were performed in defined serum-free knockout serum replacement media (KOSR)¹¹ consisting of KO-MEM, 20% knockout serum replacement, glutamine, non-essential amino acids, penicillin-streptomycin (all from Thermo Scientific, Waltham, MA, USA) supplemented with the following small molecules and growth factors: fibroblast growth factor (FGF), Rho-associated, coiled containing protein kinase inhibitor (ROCKi [Y27632]), LDN193189, SB431542, IWP3, fibroblast growth factor 8a (FGF8A), smoothened agonist (SAG), and DAPT. Cells were aggregated via centrifugation using AggreWell plates (Stem Cell Technologies) to a defined EB size of 2100 cells. After overnight culture of the cells in AggreWell plates in 37°C, 5% CO₂, EBs were collected. EBs were subsequently cultured in ultra-low attachment plates in supplemented KOSR media with small molecules, based on previous studies¹². EBs were

cultured at 37°C in 5% CO₂. Half of the media was replaced daily. On days in which the small molecule formula was changed, EBs were collected with strainers (37 µm pore size, Stem Cell Technologies) and moved to the appropriate media. After day 18 of differentiation, EBs were transferred to neural maintenance media NTD2 (neurobasal media), 1X B27, 1X insulin-transferrin-selenium (ITS), 1X pyruvate, 0.5 µg/ml cAMP, 0.4 µg/ml ascorbic acid, 25 µM BME, 25 µM glutamine (all from Thermo Scientific) and 10 ng/ml each brain-derived neurotrophic factor (BDNF), glial cell line-derived neurotrophic factor (GDNF), ciliary neurotrophic factor (CNTF), insulin-like growth factor (IGF)-1 (R&D Systems, Minneapolis, MN, USA).

Dissociation of embryoid bodies. EBs were collected on day 20 to 22 and placed into GentleMACS dissociation reagent (Miltenyi, Auburn, CA, USA) and dissociated at 37°C for 20 minutes, with gentle hand pipetting after 10 minutes. Dissociated cells were passed through a strainer, collected in NTD2 media and counted. For continued culture, cells were plated onto laminin coated coverslips in NTD2 media and cultured at 37°C in 5% CO₂. For injection, cells were resuspended at 20,000 cells per 2.5 µl in Matrigel with NTD2 media supplemented with 30 ng/ml each BDNF, GDNF, CNTF, IGF-1.

Animals

Male and female Gunn rats used in this experiment were bred in the University of Kansas Medical Center's (KUMC) colony by pairing homozygous jj males and heterozygous Nj females. Rats lived with their mothers and siblings before and after surgery and were weaned at 28 days of age (P28). Animals were housed in a temperature-controlled (23–25°C) and humidity-controlled (45–50%) room maintained on 12/12-h light/dark cycles with food (Teklad laboratory animal diets 8604; Envigo, Madison, WI, USA) and water available ad libitum. All experimental procedures were conducted in accordance with the Guide for the Care and Use of Laboratory Animals. The study was approved by the University of Kansas Medical Center's Institutional Animal Care and Use Committee (IACUC).

Bilirubin Level Measurement

Total serum bilirubin (TSB) levels of all jj rats were measured at postnatal day 17 (P17). For each animal, about 50 µl of blood was taken and the TSB concentration was determined using a Leica Unistat bilirubinometer (Reichert Inc., Depew, NY, USA). Bilirubin levels in Nj rats were below the limit of detection of the bilirubinometer.

Surgery

At 21 days of age (P21), rats were anesthetized with isoflurane (3–4% for induction and 2–2.5% for maintenance with oxygen) and placed in a stereotaxic frame (Kopf, Tujunga,

CA, USA). A small hole on the skull was drilled over the GP using stereotaxic coordinates from a developing rat brain stereotaxic atlas¹³. Coordinates were 5.3 mm anterior and 2.8 mm lateral from the interaural midpoint. A 26-gauge, 10- μ l Hamilton microsyringe was lowered to a depth of 5.0 mm from the brain surface and NPCs suspended in Matrigel (20,000 in 2.5 μ l) were injected into the GP unilaterally at a flow rate of 0.5 μ l/min. The needle was left in place for an additional 5 min to prevent cell efflux and then slowly removed. In order to compare time course and regional influence of cell development, a subgroup of jj rats received bilateral NPCs: one side in the striatum (coordinates: anterior-posterior: 6.5 mm, medial-lateral: 2.8 mm, dorsal-ventral: 5.0 mm), and the other side in the GP. After surgery, the scalp was sutured and the rat was returned to its cage for recovery. All rats received ketoprofen 5 mg/kg subcutaneously for 3 days. As planned, an immunosuppressant was not used in this experiment.

Immunohistochemistry and Immunocytochemistry

At 3 weeks post-cell transplantation (P42 or P43), rats were deeply anesthetized with isoflurane and transcardially perfused with ice-cold phosphate-buffered saline (PBS) followed with 4% paraformaldehyde (PFA; Sigma-Aldrich, St. Louis, MO, USA). Brains were removed and cryoprotected in 30% sucrose PBS solution prior sectioning for immunohistochemistry (IHC) analyses. Subgroups of double-grafted jj rats were only allowed to survive 3 or 10 days after NPC grafting. Coronal sections containing the graft and the GP were cut at 30 μ m with a cryostat (Leica CM3050 S). All sections were processed with standard floating section methods. Every sixth section was stained with mouse monoclonal antibody specific for human species cytoplasmic marker, STEM121 (1:500; Cellartis-Clontech, Mountain View, CA, USA), to identify grafted human cells and alternatively double stained with the following antibodies: rabbit anti-human Ku80 (1:500; ABC am, Cambridge, MA, USA) for human cell nuclei, rabbit anti-parvalbumin (PV, 1:200; PyroXenitic, Rosemont, IL, USA) or goat-anti-PV (1:500; SantaCruz, Dallas, TX, USA) to identify graft cells expressing PV, rabbit anti-proenkephalin (PENK, 1:1000; LifeSpan BioSciences, Seattle, WA, USA) for graft or host cells expressing PPE. A further set of 1:6 series sections was processed for double staining of mouse anti-STEM123 (1:300; specific for human glial fibrillary acidic protein (GFAP); Cellartis-Clontech) and Ku80. Extra cultured cells that were not used for transplantation were plated onto laminin and fixed after 30 min or 6 days of continued culture; immunocytochemistry (ICC) was performed to identify the cell properties. The following antibodies were used for ICC: mouse immunoglobulin G (IgG)2A anti-glutamic acid decarboxylase 6 (GAD-6, 1:100; Developmental Studies Hybridoma Bank, University of Iowa, Iowa City, IA, USA), rabbit anti- β III-tubulin (1:200; ECM

Bioscience, Versailles, KY, USA), goat-anti-PV (1:500; SantaCruz), rabbit anti-proenkephalin (PENK, 1:1000; LifeSpan BioSciences, Seattle, WA, USA), and mouse anti-STEM123 (1:300; Cellartis-Clontech). Immune reactions were visualized by corresponding secondary antibody labeling: goat anti-mouse IgG (H+L) Alexa Fluor 488 (1:2,000; Invitrogen, Waltham, MA, USA), goat anti-rabbit Alexa Fluor 555 (1:2000; Invitrogen), cyanine 3 (Cy3) donkey anti-goat IgG (1:200; Jackson Immuno Research, West Grove, PA, USA), goat anti-mouse IgG2A Alexa Fluor 594 (1:1000; Invitrogen).

Quantification and Statistics

All sections were examined under a fluorescence microscope (Nikon Eclipse 80i; Nikon, Melville, NY, USA) and analyzed with CellSens Standard (Olympus, Center Valley, PA, USA) or NIS-Elements AR (Nikon) software. Images (2 \times , 4 \times , 10 \times , and 20 \times) of the grafted areas were used. Based on the STEM121 and Ku80 double labeling, the numbers of viable transplanted cells were manually counted with CellSens or NIH ImageJ (NIH, Bethesda, MD, USA) independently by two people. The mean was multiplied by 6 to estimate the total number of viable cells. The migration distances of grafted cells from the graft tract and the length of outgrowth axons were measured with CellSens Standard or NIH ImageJ based on the images of 10 \times magnification. Cell survival rates between groups were analyzed using analysis of variance or Student's *t* test (when there were only two groups to compare), and Pearson's product moment correlation was used for the correlation between bilirubin levels and graft cell survival rates (SigmaStat 4.0, Systat Software Inc., San Jose, CA, USA). Statistical significance was set at $p < 0.05$. All data are shown as mean \pm standard error of the mean.

Results

Characteristics of the hESC-derived MGE-like NPCs

Cells cultured for 30 min or 6 days after transplantation were examined with ICC in vitro to identify their neurochemical phenotype. The results indicated that a large proportion of cells were GABAergic, as assessed by expression of GAD-6 in both 30 min and 6 days culture. Cells in which colocalization of GAD-6 and β III-tubulin were identified were abundant; some cells also co-expressed GAD-6 and PV, or GAD-6 and PENK, indicating cells differentiated into MGE GABAergic neuron-like phenotypes. In cells that were cultured for 6 days after EB dissociation, rich, extended long fibers were observed (Figure 1). ICC to detect GFAP (using STEM123 antibody) showed that $\sim 45\%$ of the cells differentiated into astrocytes. ICC to detect acetyltransferase was negative, suggesting no cholinergic cells in the culture (data not shown).

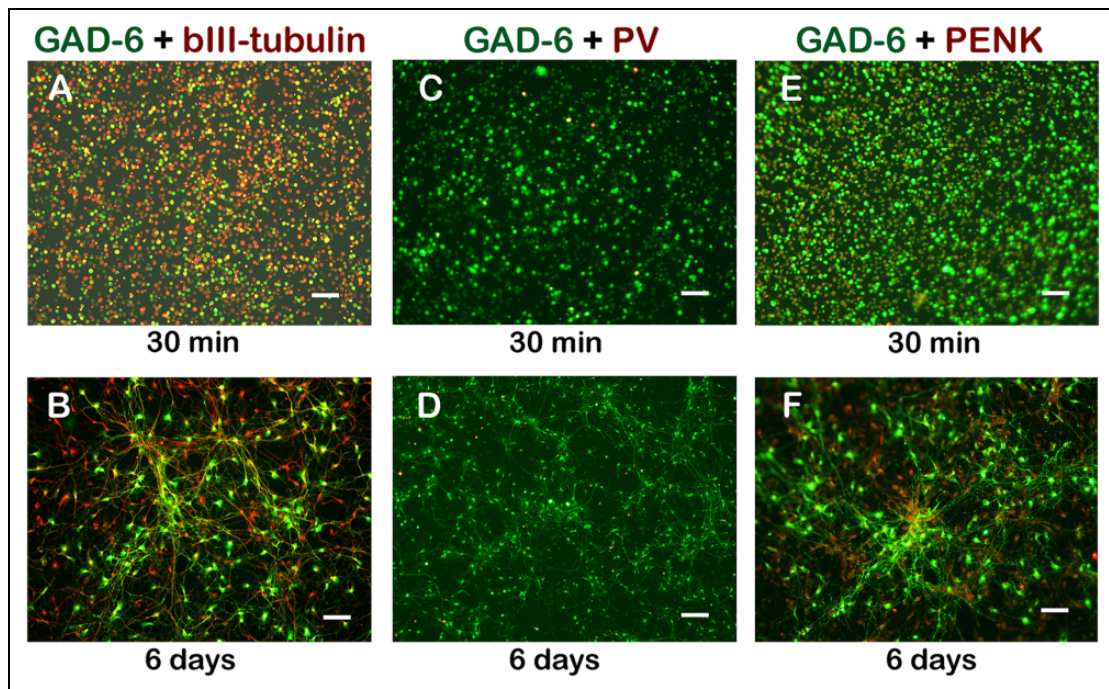


Figure 1. MGE-like NPCs expressed GAD-6, PV, and PENK in culture. Photomicrograph showing most of the cells were GAD-6-ir and β III-tubulin-ir ((a): 30 min; (b): 6 days) indicating a GABAergic phenotype. GAD-6 and PV double labeling show a subgroup of GABAergic neurons also expressed PV ((c): 30 min; (d): 6 days). GAD-6 and PENK double labeling indicated many GABAergic neurons were PENK-ir cells ((e), 30 min; (f), 6 days). Scale bar: a–f, 50 μ m; d, 100 μ m. GABA: gamma-aminobutyric acid; GAD-6: glutamic acid decarboxylase-6; MGE: medial ganglionic eminence; NPC: neural progenitor cell; PENK: proenkephalin; PV: parvalbumin.

Survival of the MGE cell-like NPCs 3 Weeks Post-Transplantation

Surviving grafts were identified in brains of all transplanted rats. Cell survival rate was calculated as a percentage of the number of Ku80-ir nuclei surrounded by or apposite to STEM121-ir cells to the total number of cells injected. Cell survivability 3 weeks post-transplantation was 2.7% (527 ± 187) in the jj group and 0.8% (152 ± 66) in the Nj group. The survival rate of transplanted cells was significantly greater in the jj brain than in the Nj brain ($T=53.0$, $p=0.026$) (Figure 2). IHC for STEM123 and Ku80 labeling did not identify cells expressing STEM123 in the graft of either jj or Nj brains (data not shown).

Cell Distribution and Neurite Outgrowth 3 Weeks Post-Transplantation

The anterior-posterior distance of transplanted cells' distribution was defined by the presence of cells stained with both STEM121 and Ku80. The cell distribution in the jj group was $1620 \pm 167.6 \mu$ m and $930 \pm 142.6 \mu$ m in the Nj group. Most of the grafted cells were located within a short distance (50–100 μ m) of the injection track. Cell clusters were usually observed at the interface of the graft tract and the host tissue. Depending on the site of the injection tract, small groups or single cells spread in a wide range. Grafted cells were

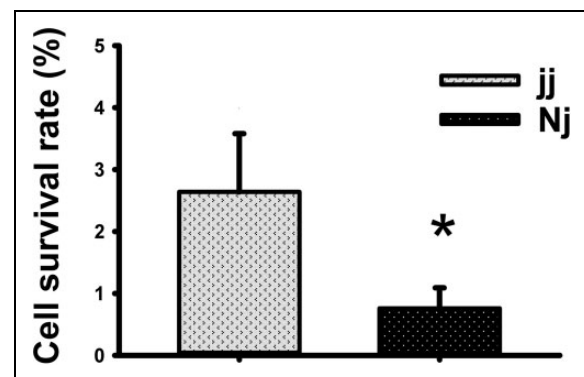


Figure 2. Survival of grafted MGE-like NPCs in jj and Nj brain. Grafted cell survival rate was significantly higher in jj brain than in Nj brain. Without immunosuppressant, survival rate was 2.7% in jj, but only 0.8% in Nj brain;

*indicates statistical significance ($p < 0.05$).

jj: jaundiced; MGE: medial ganglionic eminence; Nj: non-jaundiced; NPC: neural progenitor cell.

identified mainly in the GP and internal capsule (ic), but some cells were located in the basal nucleus, stria terminalis (ST), bed nucleus of the stria terminalis (BNST), the ventral portion of the thalamus, and the lateral ventricle (lv). In the dorsal and anterior parts of the graft, scattered cells could be seen in the cerebral cortex, corpus callosum (cc), and striatum (str). Necrotic cells were observed in both jj and Nj

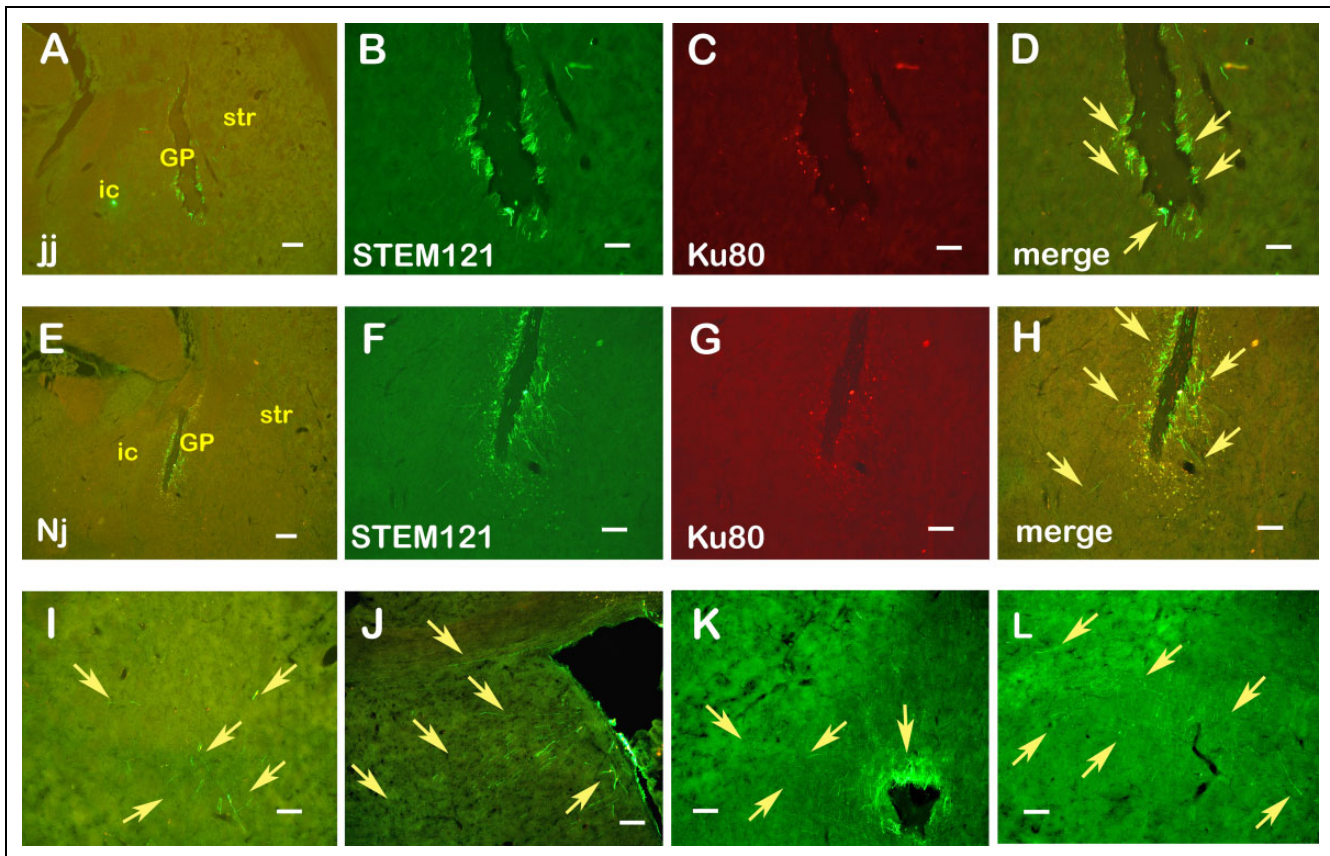


Figure 3. Grafted MGE-like NPC survival and fiber outgrowth in jj and Nj brain 3 weeks post-transplantation. (a–h): IHC staining for STEM121 and Ku80 confirmed grafted cell survival along the injection track in the GP and ic area. Note that most of the surviving cells were in the graft/host border, or migrated into the host parenchyma. Outgrowth fibers distributed densely near the host-tract interface. In both brains, many short, parallel fibers can be found along the edge of the tract. (a–d): jj brain; (f–h): Nj brain (a and h are lower magnification to show the location of the graft). (i): Neurons migrated away from the tract in the GP and striatum. Note that there were long fibers with semi-perpendicular collaterals. (j): Cells that grew into the lateral ventricle generated long fibers projecting medially toward the septal area. Long fibers extending into the corpus callosum can also be seen. (k): Graft in the GP/ic intersection. Short parallel fibers aggregated in the dorsal edge of the track; thin, long fibers extended medially and ventrally to the thalamus. (l): Photo from the same plane as (k), ventromedial side, showing long, thin projection fibers with semi-perpendicular collaterals growing into the thalamus and subthalamic areas. Scale bar: (a and e), 200 μ m, the others 100 μ m. Arrows point to representative cells and fibers. GP: globus pallidus; ic: internal capsule; IHC: immunohistochemistry; jj: jaundiced; MGE: medial ganglionic eminence; Nj: non-jaundiced; NPC: neural progenitor cell.

brains, especially along the dorsal portion of the graft track. There were more necrotic tissue and fewer surviving cells in the Nj than jj brains (see Figure 3 (a–h) for representative images of graft survival in jj and Nj brain).

Neuritic outgrowth was observed a greater distance from grafts than cell distribution. In the jj group, neuritic outgrowth occurred primarily in an anterior-posterior distance of $2070 \pm 61.5 \mu\text{m}$. For the Nj group the distance was $1560 \pm 110.6 \mu\text{m}$. Abundant fiber outgrowth was observed from grafts in jj and Nj brains; usually the closer to the injection site the denser the fibers. Most fibers were distributed in the GP and the ic. Fibers extending into the BNST, the ST, reticular thalamic nucleus, lateral anterior nucleus of the thalamus (VA), or ventral lateral nucleus of the thalamus (VL) were frequently observed. In more posterior sections, some fibers were found in the

entopeduncular nucleus or the lateral hypothalamic area. When cells grew into the lateral ventricle, fibers were observed in the septal area and fornix (Figure 3(j)). Morphologically, a large population of grafted cells featuring short, thick parallel fibers was identified. These were especially prevalent when cells distributed along the border of the track and the host parenchyma (see Figure 3(d, h, k)). We also frequently observed a number of long, thin fibers from the GP/ic area, extending parallel medially and/or ventrally toward the thalamus and subthalamic areas and forming specific projection patterns; some of this type of long fibers had semi-perpendicular collaterals (Figure 3(i,l)). Graft cells always extended their fibers toward the host tissue. We observed no fibers extending across the tract to the other side of the host parenchyma. Moreover, very few long fibers projected laterally into the striatum.

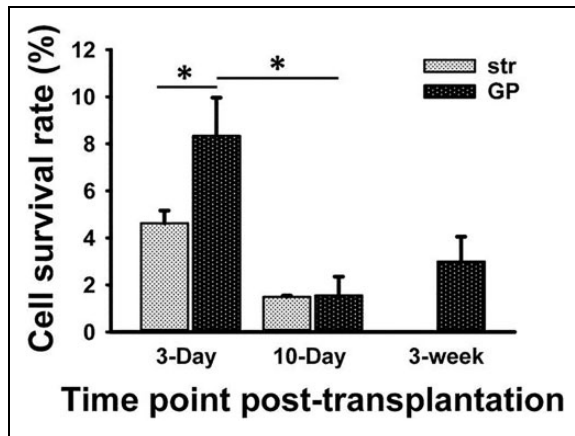


Figure 4. MGE-like NPC survivability when grafted into striatum or GP at 3 days or 10 days post-transplantation. Overall, cell survival rate was significantly greater at 3 days. At 3 days, graft survival rate was greater for the GP than the striatum. Survival rate did not differ between the GP and striatum at 10 days. Cell survivability was maintained in a low yet stable rate from 10 days to 3 weeks post-transplantation.

Early Time Course of Graft Cells' Survival and Development – 3 days and 10 Days Post-Transplantation

The survival and growth of MGE-like NPCs grafted into striatum or GP of jj brains were measured 3 and 10 days after transplantation. In the 3-day group, the cell survival rate was 8.4% (1668 ± 324) in the GP and 4.6% (924 ± 108) in the striatum. However, 10 days after grafting, cell survivability reduced to 1.55% (300 ± 159) in the GP and 1.49% (297 ± 9) in the striatum. Cell survivability was significantly greater 3 days than 10 days post-transplantation ($F(1,4)=27.78$, $p=0.006$). There was no difference between graft sites ($F(1,4)=3.09$, $p=0.154$) nor was there an interaction between time-point and graft site ($F(1,4)=3.81$, $p=0.123$). Post-hoc analyses with the Holm–Sadako method further revealed greater survival rates at 3 days compared with 10 days in the GP ($t=5.1$, $p=0.007$), but not in the striatum ($t=2.353$, $p=0.078$). Moreover, graft survival rate was greater in GP than in striatum only at 3 days post-transplantation ($t=2.792$, $p=0.049$) (Figure 4). Brain regions where grafted cells distributed 3 days or 10 days post-transplantation were similar to what we observed 3 weeks post-transplantation. At these two early time-points, most surviving cells were located inside the graft track, with few cells having migrated into the host tissue. This was especially true 3 days post-grafting. Most cells that survived inside the track were small and lacked cell processes. Single cells or cell clusters which migrated into the host parenchyma or aggregated in the host-graft border usually had fiber outgrowth. Even at the 3-day time-point, there were long fibers identified in the striatum and cc. At 10 days after transplantation, a few short, thick, parallel fibers and some

long projections from the GP to the ic and the thalamus were observed (Figure 5).

Bilirubin Level in jj Rats and its Correlation to Cell Survival

TSB concentration was 13.81 ± 0.39 mg/dl. Pearson product moment correlation revealed no correlation between the TSB and cell survival rates in the GP of jj rats ($r=-0.391$, $p=0.263$).

Parvalbumin Expression in Transplanted hESC-derived MGE-like NPCs

IHC double labeling for PV and STEM121 revealed low numbers of PV-ir grafted MGE-like grafts in the jj host GP and striatum 3 days and 10 days post-transplantation. Similarly, very few PV-ir graft neurons were found in both jj and Nj brains 3 weeks post-transplantation. Most of the PV-ir neurons were identified in the graft tract and the size of the cells was relatively small. The number of cells in tissue was much less than that in cell culture (Figure 6).

PENK Expression in the Host Brain

Although ICC indicated substantial PENK-ir NPCs in the cell culture, IHC of PENK and STEM121 double labeling showed no definitive PENK-ir grafted neurons in the brain at 3 days, 10 days, or 3 weeks after transplantation. Instead, strong PENK-ir fibers and cells, originating from the host tissue, aggregated and surrounded the graft in both jj and Nj brains. Interestingly, at 10 days and 3 weeks post-transplant, when the site of the graft was in or adjacent to the GP, there were PENK-ir fibers extending from the GP to the region where surviving grafted cells and fibers were located. Three days after transplantation, PENK-expressing cells appeared surrounding the track and graft, but the labeling was not as strong as that in 10 days and 3 weeks. In addition, there was a distinct zone with less PENK-ir staining between the graft and the high PENK-expression area. This zone was not observed in brains 10 days or 3 weeks after grafting (Figure 7).

Discussion

Our ultimate goal is to use cell therapy to ameliorate dystonia in kernicterus by restoring GP and basal ganglia circuit function. The NPCs we chose for transplantation were differentiated into MGE-derived progenitors, the major origin of GP neurons⁹. However, MGE progenitors have multiple targets, and GP is not their only destination^{12,14}. To identify whether the characteristics of these cells met the basic requirements for transplantation, we used ICC to co-label GAD-6 and β III-tubulin to validate the presence of GABAergic neurons in culture. Using our method modified

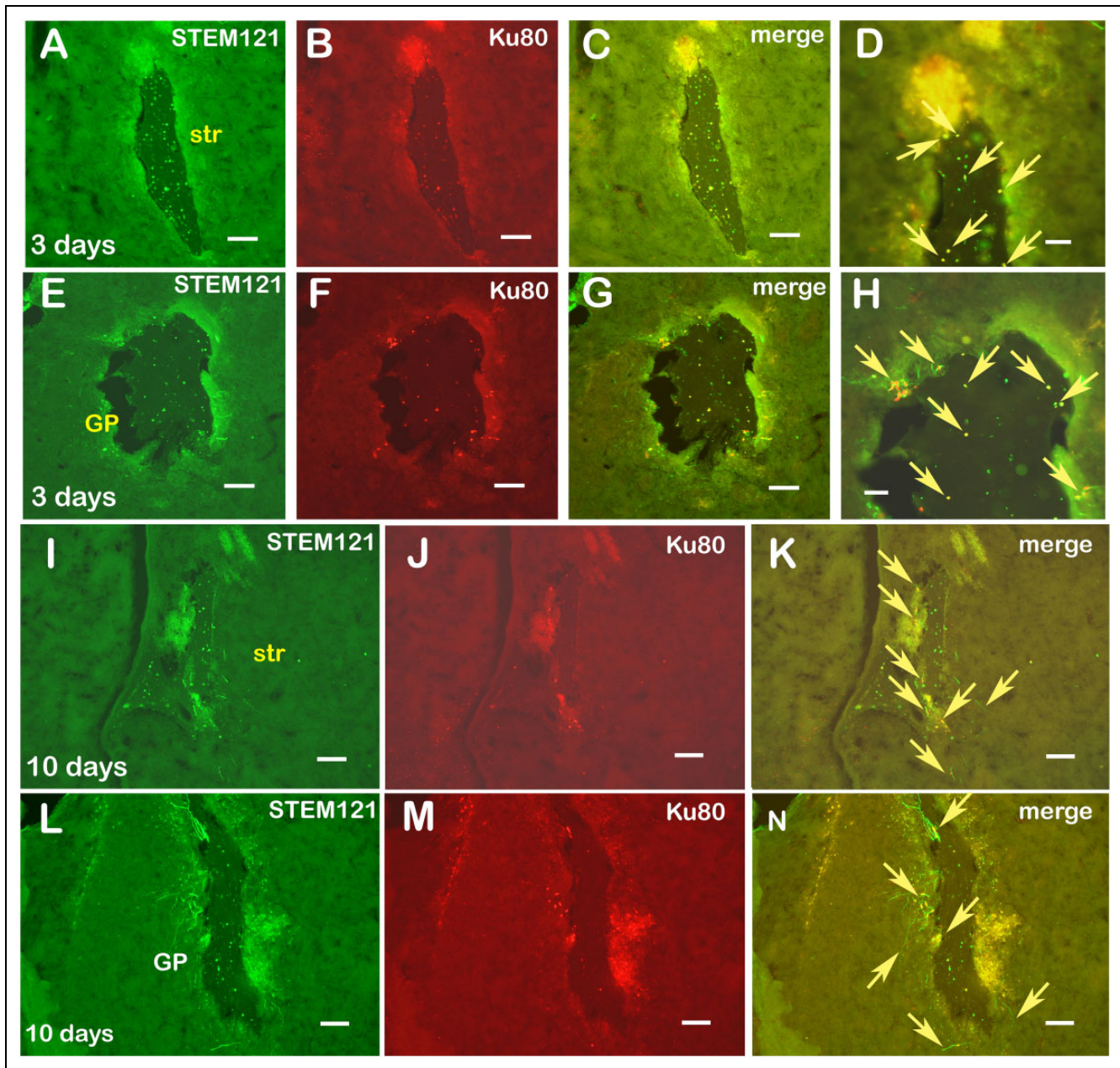


Figure 5. Grafted MGE-like NPCs survived and grew neurites in *jj* brain at 3 days (a–h) and 10 days (i–n) post-transplantation. IHC of STEM121 and Ku80 co-labeling showing many surviving cells in the tract, most of them had no cell process. Few cells attached to the host tissue started to grow short fibers. (a–d): striatum. (e–h): GP. (d) and (h) are shown at higher magnification to show the cells remained in the tract. IHC of STEM121 and ku80 at 10 days post-transplantation indicated more cells migrated to the host parenchyma; these cells usually had fiber outgrowth. The number of surviving cells was less at 10 days than at 3 days. (i–k): striatum; (l–n): GP. Necrotic cells were observed at both 3 days and 10 days. Scale bar: (d, h) 50 μ m, all the others 100 μ m. Arrows point to representative cells and fibers.

GP: globus pallidus; MGE: medial ganglionic eminence; NPC: neural progenitor cell; str: striatum; GP: globus pallidus; IHC: immunohistochemistry; *jj*: jaundiced; MGE: medial ganglionic eminence; NPC: neural progenitor cell; str: striatum.

from Kim¹², the majority of the cells were GABAergic neurons. ICC for GAD-6 and PV double staining further confirmed that a subgroup of GABAergic neurons also expressed PV. This is important because up to 60% of neurons of the GP are PV-expressing neurons^{8,9,15}. Our result

was similar to what was previously reported¹². We also found many cultured cells that co-expressed GAD-6 and PENK, a result that has not been documented before. PENK-expressing GABAergic neurons exist in both GP and striatum^{8,16}.

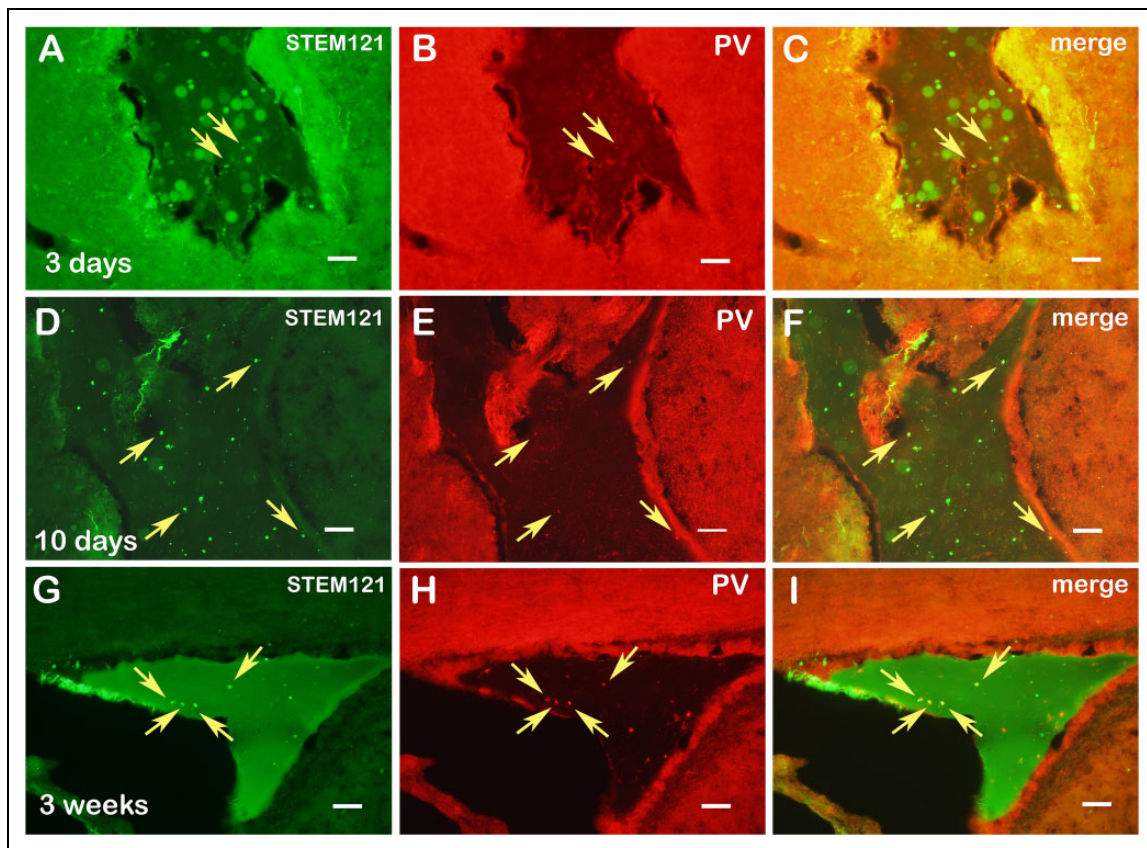


Figure 6. PV expression in the grafted MGE-like NPCs. IHC labeling for PV and STEM121 indicating PV-ir grafted neurons in the GP, striatum, and lateral ventricle at 3 days, 10 days, and 3 weeks post-transplantation. Most of the PV neurons were identified in the graft tract; the percentage of PV-ir cells was less than in cell culture. (a–c): jj GP, 3 days post-transplantation; (d–f): Nj striatum, 10 days post-transplantation; (g–i): jj ventricle, 3 weeks post-transplantation. Scale bar: 100 μ m. Arrows point to representative cells. GP: globus pallidus; IHC: immunohistochemistry; jj: jaundiced; MGE: medial ganglionic eminence; Nj: non-jaundiced; NPC: neural progenitor cell; PV: parvalbumin.

We found that WA09 cell line-derived MGE-like NPCs survived at least 3 weeks post-transplantation without immunosuppressant and formed neurites with extensive outgrowth in the GP and its adjacent structures in jj and Nj rat brains. Moreover, the graft survivability was significantly greater in the jj brain. These findings agree with our previous study, which showed that hESC-derived excitatory NPCs had a greater survival rate when transplanted into jj than Nj brain⁶. The hypotheses that slightly elevated bilirubin exerted antioxidant¹⁷ and immunosuppressant¹⁸ effects that protected graft survival were further supported by our current results.

It is notable that the survival rates of the excitatory spinal interneurons grafted in the striatum (21% in jj and 12.4% in Nj) in our previous study⁶ were much higher than the survival rates of the MGE-like NPCs (2.7% in jj and 0.8% in Nj) grafted into the GP. While the cell type can play a role in survivability, site of transplantation could also affect the result. To clarify this possibility, we used a subgroup of jj rats that received MGE-like NPC grafts in one striatum and in the contralateral GP to compare the graft survival and development at two very early time-points: 3 days and 10 days after transplantation. Taken together with our previous

results, we believe that cell type is a more important factor for survivability than graft site at these time-points. The main factor that influenced cell survival rate was the post-graft time-point. It was not surprising that the survival rate was higher at 3 days, since the immune response likely had not reached its peak at this time-point. However, the survival rate of the 10-day group was similar to that of the 3-week group. This suggests that bilirubin may have mitigated an immune response. TSB levels increase from P10 until they reach a maximum around P15 or P16, at which time they gradually decrease around P17 to P19 but remain higher in jj rats even at D60^{19,20}. Due to its immunosuppressant properties, slightly greater bilirubin levels may have contributed to a comparable survival rate in the graft 10 days and 3 weeks after the transplantation. In addition, the fact that graft survival rate was greater in the GP than that in the striatum 3 days, but not 10 days, post-transplantation further suggests a protective effect of bilirubin, especially in this bilirubin-sensitive part of the brain^{3,21}.

The lack of correlation between TSB at D17 and NPC survival rates suggests that TSB levels are a poor predictor of graft survival. The low variability of TSB may have

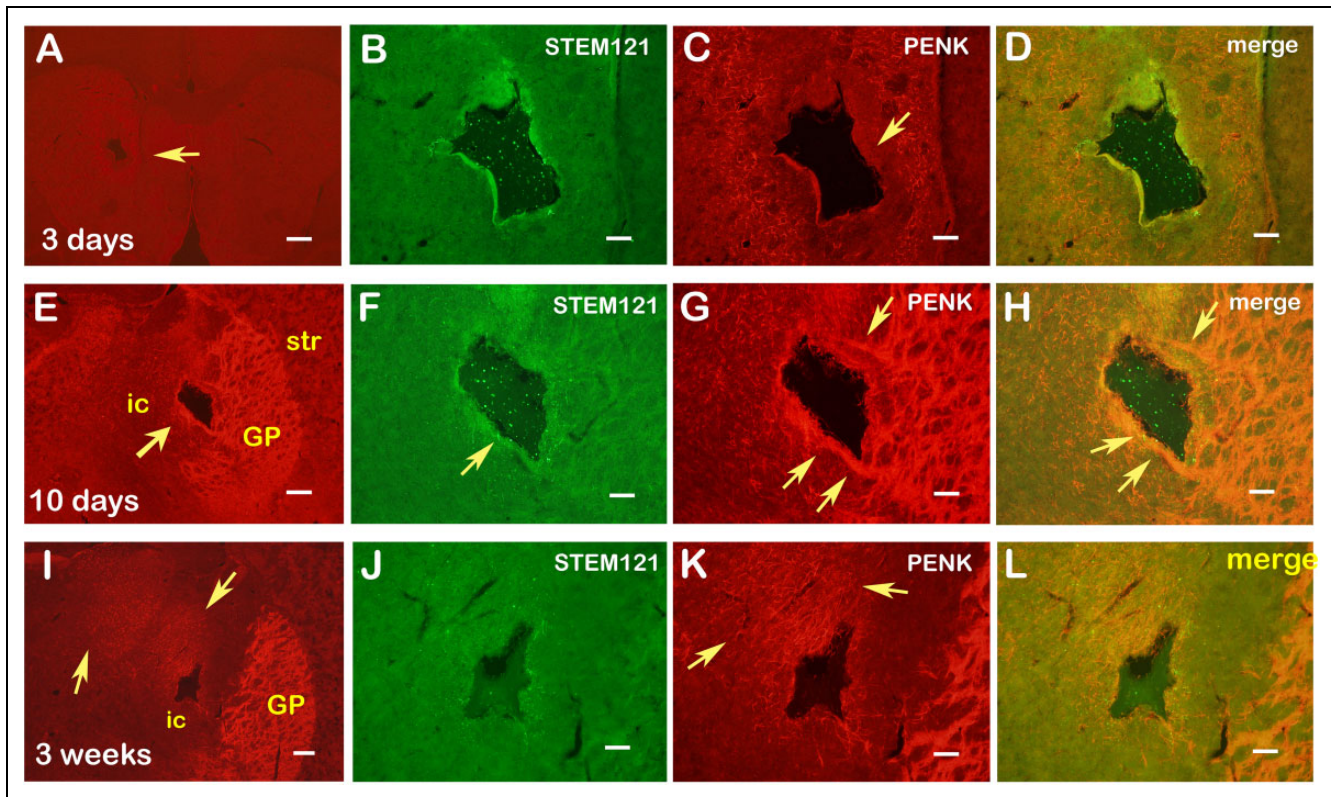


Figure 7. PENK expression in host brain. IHC revealed strong PENK expression in MGE-like NPC grafts, included glia and connecting fibers, at or near the graft site in the host brain. (a–d): 3 days post-transplantation in the striatum. PENK-expressing astrocytes surrounded the graft track. There was a zone of low PENK expression between the graft and the surrounding PENK-expressing astrocytes. (e–h): 10 days post-transplantation in the GP. The graft was located between the GP and ic (note that PENK fibers extended from the GP toward the region containing surviving graft cells and fibers). There were also PENK-expressing astrocytes near the graft site. (i–l): 3 weeks post-transplantation in the GP. In this plane, the actual graft location was between the ic and thalamus. Note the PENK-expressing astrocytes were dorsomedial to the graft, included a large area of the thalamus. (a, e, i): lower magnification to show the location of graft and area containing PENK-expressing cells and fibers. Scale bar: (a), 500 μm , (e, i), 200 μm ; all the others 100 μm . Arrows point to graft location, PENK-expressing host cells, fibers, and regions. GP: globus pallidus; ic: internal capsule; IHC: immunohistochemistry; MGE: medial ganglionic eminence; NPC: neural progenitor cell; PENK: proenkephalin; str: striatum.

contributed to this lack of correlation. However, TSB does not reflect the free bilirubin concentration in the brain²⁰. The fact that graft cells survived better in the jj brain suggests that bilirubin played a necessary but not sufficient role in graft survival. Although the strategy of not using immunosuppressant may have revealed a protective effect of bilirubin on graft survival, the overall survival rate was low. This suggests that immunosuppressant may be necessary to improve survival.

Graft cells and their fibers were identified by STEM121 and Ku80 IHC labeling. Although most of the cells were preferentially located near the graft core area, many graft cells migrated a greater distance. We found that when graft cells attached to the ventricle walls, they usually survived and grew abundant fibers (Figure 3(j)) perhaps due to nutrition supplies from the cerebrospinal fluid and greater space to grow. However, this conflicts with another report of worse graft survival near the ventricle due to immune factors²². Notably, in contrast to the condition 3 weeks after

transplantation in which most surviving cells were found in the graft–host border or had migrated into host tissue, there were more surviving cells inside the graft track at two earlier time-points (especially 3 days). Fewer cells migrated into the host tissue. The cells remaining in the track were small and had no outgrowth of cell processes, indicating they were still in an immature neuroprogenitor state. A similar condition was reported even at 3 weeks after transplantation in a study using hESC-derived NPCs grafted into mouse brain²³. The fate of these immature cells may depend on their phenotype and their opportunity to integrate with host tissue, since there were few surviving cells in the graft track 3 weeks after transplantation.

We identified two distinct morphological patterns of fiber outgrowth and distribution in both jj and Nj brains. One pattern was characterized by short and thick parallel fibers, which usually had cell bodies nearby. This pattern was observed in most of the grafted brains and was very easy to recognize along the host-injection tract interface. This

type of fiber arrangement resembled the dendrites of PV neurons in the GP⁷, which receive PENK projections from striatal medium spiny neurons. Further investigation is necessary to test whether our fibers share this phenotype. Another frequently observed pattern was a population of medial and ventral-directed long axons, which projected to the thalamus or regions ventral to the thalamus. Since these areas are the targets, or pass-through sites to the targets, of GP output pathways^{7,15}, it may be that the grafted neurons formed normal GP efferent fibers projecting to multiple targets. Interestingly, long fibers projecting to the striatum, another destination of the GP circuit⁸, were not found. It was reported that GP neurons were dichotomous: those GP neurons projecting to the thalamus, subthalamic nucleus (STN), or substantia nigra (SN) were PV-positive prototypic GABAergic neurons, while the projections to the striatum were from PENK-positive arypallidal neurons^{8,15}. Our observations suggest one of two possibilities: either the grafted cells had not differentiated enough to represent certain GP cell types, or some types of grafted cells did not adapt to the host environment and thus did not survive.

Although numerous PV-ir cells were co-labeled with GAD-6 in culture, few MGE-like NPCs expressed PV after transplantation. The ones that did remained in the Matrigel of the injection tract. One possibility is that the development of these cells was delayed after grafting and did not express the more mature phenotypic marker within our time frames. A similar outcome was reported in another stem cell transplantation study in a rat model of Huntington's disease²⁴. However, this could also suggest that some PV-ir cells may have down-regulated PV expression when they migrated into host tissue. Because PV-ir neurons are the largest cell type in the GP^{7,15} and they are decreased in kernicterus²⁵, improving grafted PV neuronal survival and function will be important for stem cell therapy in kernicterus.

Despite a large number of PENK-ir cells in culture, PENK-ir cells were not found in either jj or Nj brain. This population of cells may not have survived or may have lost their PENK phenotype after transplantation. We did, however, observe PENK-ir fibers (Figure 7) extending from the host GP to the graft. These fibers should be axon collaterals from striatal PENK-ir medium spiny neurons, which normally synapse with GP neurons¹⁶. This result suggests that MGE-like NPC grafts may attract striatal medium spiny neuron collateral fibers growing toward it, which is vital for reconstructing impaired circuits. Surprisingly, the grafts induced strong PENK expression near every graft site of the host brain. Their shape suggests that these PENK-ir cells could be astrocytes. The aggregation and over-expressing of PENK in host astrocytes has not been documented previously. A role for PENK in astrocytes has been proposed for modulating brain development and maturation^{26,27}. Because PENK has been considered to be a negative trophic regulator for neuronal proliferation and differentiation, the interaction between the PENK-expressing astrocytes and opioid receptor-expressing neurons may be a mechanism for

affecting growth and migration of these neurons²⁶. The PENK-hyper-expressing astrocytes that we observed could be guiding the graft cells. Further research is necessary to test this hypothesis.

In conclusion, the present study demonstrated hESC-derived MGE-like NPCs were able to survive and generate abundant and diverse fiber types within a short period after being transplanted into jj or Nj rat brain. These grafted cells have the potential to form circuits between the GP and its connecting nuclei. It will be necessary to extend our time-points to determine synaptic formation and other aspects of NPC development²³. The graft survival rate was greater in jj than in Nj rats, which could be due to the slightly elevated bilirubin concentration in the jj brain. The overall cell survivability was low however, indicating immunosuppressant may be necessary to increase graft survival. In addition, compared with other studies^{23,24}, the total number of cells injected was low in our experiment. Increasing the injected cell number could increase the number of surviving cells in future studies. Because we only focused on the anatomical aspects of cell survival and development in jaundiced rats, future studies are required to examine functional recovery in dystonic rats and to explore underlying mechanisms of recovery.

Various types of stem cells have been widely tested in many animal models of Parkinson's disease^{28,29}, Huntington's disease^{24,30}, and other neurological conditions that affect motor function^{31,32}. To our knowledge, there have been no preclinical studies in which stem cells were transplanted into the GP to treat dystonia. There have also been no studies reporting NPCs specifically designed to differentiate into GP neurons. The results of this research suggest the possibility of using hESC-derived MGE-like NPCs for repairing GP neurons. With further optimization of the differentiation protocol, these cells hold promise for use in restoring basal ganglia circuits in kernicterus.

Acknowledgements

The authors would like to acknowledge Sarah Tague, PhD and Jing Huang, BS of the Integrative Imaging Center for their technical assistance and the Transgenic and Gene Targeting Institutional Facility at the University of Kansas Medical Center for preparation of differentiated cells.

Ethical Approval

This study was approved by the University of Kansas Medical Center institutional animal care and use committee (IACUC).

Statement of Human and Animal Rights

Animals used in this study were treated according to the National Research Council's Guide for the Care and Use of Laboratory Animals.

Statement of Informed Consent

Statement of Informed Consent is not applicable.

Declaration of Conflicting Interests

The authors declared no potential conflicts of interest with respect to the research, authorship, and/or publication of this article.

Funding

The authors disclosed receipt of the following financial support for the research and/or authorship of this article: The Transgenic and Gene Targeting Institutional Facility at the University of Kansas Medical Center Facility is supported by NIH Center of Biomedical Research Excellence program project P20 GM104936. This work was supported by Children's Mercy Hospital, the Ronald D. Defenbaugh Foundation, and the Kansas Intellectual and Developmental Disabilities Research Center (KIDDDRC) center grant HD090216.

References

1. Watchko JF, Tiribelli C. Bilirubin-induced neurologic damage – Mechanisms and management approaches. *N Engl J Med.* 2013; 369(21):2021–2030.
2. Shapiro SM. Definition of the clinical spectrum of kernicterus and bilirubin-induced neurologic dysfunction (BIND). *J Perinatol.* 2003;25(1):54–59.
3. Shapiro SM. Bilirubin toxicity in the developing nervous system. *Pediatr Neurol.* 2003;29(5):410–421.
4. Gunn CK. Hereditary acholuric jaundice in a new mutant strain of rats. *J Hered.* 1938;29(4):137–139.
5. Johnson L, Sarmienyo F, Blanc WA, Day R. Kernicterus in rats with an inherited deficiency of glucuronyl transferase. *AMA J Dis Child.* 1959;97(5, Part 1):591–608.
6. Yang FC, Riordan SM, Winter M, Gan L, Smith PG, Vivian JL, Shapiro SM, Stanford JA. Fate of neural progenitor cells transplanted into jaundiced and nonjaundiced rat brains. *Cell Transplant.* 2017;26(4):605–611.
7. Kita H. Parvalbumin-immunopositive neurons in rat globus pallidus: a light and electron microscopic study. *Brain Res.* 1994;657(1-2):31–41.
8. Mallet N, Micklem BR, Henny P, Brown MT, Williams C, Bolam JP, Nakamura KC, Magill PJ. Dichotomous organization of the external globus pallidus. *Neuron* 2012;74(6): 1075–1086.
9. Nóbrega-Pereira S, Gelman D, Bartolini G, Pla R, Pierani A, Marín O. Origin and molecular specification of globus pallidus neurons. *J Neurosci.* 2010;30(8):2824–2834.
10. Thomson JA, Itskovitz-Eldor J, Shapiro SS, Wanta MA, Swiergiel JJ, Marshall VS, Jones JM. Embryonic stem cell lines derived from human blastocysts. *Science* 1998;282(5391): 1145–1147.
11. Galvin-Burgess KE, Trvis ED, Pierson KE, Vivian JL. TGF- β superfamily signaling regulates embryonic stem cell heterogeneity: Self-renewal as a dynamic and regulated equilibrium. *Stem Cells.* 2013;31(1):48–58.
12. Kim TG, Yao R, Monnell T, Cho JH, Vasudevan A, Koh A, Kumar PT, moon M, Datta D, Bolshakov VY, Kim KS, Chung S. Efficient specification of interneurons from human pluripotent stem cells by dorsoventral and postrocaudal modulation. *Stem Cells.* 2014;32(7):1789–1808.
13. Sherwood NM, Timiras PS. A stereotaxis atlas of the developing rat brain. Berkeley: C.W.C. Education Information Center University of California Press; 1970.
14. Olsson M, Björklund A, Campbell K. Early specification of striatal projection neurons and interneuronal subtypes in the lateral and medial ganglionic eminence. *Neuroscience* 1998; 84(3):867–876.
15. Oh YM, Karube F, Takahashi S, Kobayashi K, Takada M, Uchigashima M, Watanabe M, Nishizawa K, Kobayashi K, Fujiyama F. Using a novel PV-Cre rat model to characterize pallidonigral cells and their terminations. *Brain Struct Funct.* 2017;222(5):2359–2378.
16. Shivers BD, Harlan RE, Romano GJ, Howells RD, Pfaff DW. Cellular localization of proenkephalin mRNA in rat brain: gene expression in the caudate-putamen and cerebellar cortex. *Proc Natl Acad Sci USA.* 1986;83(16):6221–6225.
17. Sedlak TW, Saleh M, Higginson DS, Paul BD, Juluri KR, Snyder SH. Bilirubin and glutathione have complementary antioxidant and cytoprotective roles. *Proc Natl Acad Sci.* 2009;106(13):5171–5176.
18. Liu Y, Li P, Lu J, Xiong W, Oger J, Tetzlaff W, Cynader M. Bilirubin possesses powerful immunomodulatory activity and suppresses experimental autoimmune encephalomyelitis. *J Immunol.* 2008;181(3):1887–1897.
19. Daood MJ, McDonagh AF, Watchko JF. Calculated free bilirubin levels and neurotoxicity. *J Perinatol.* 2009;29(Suppl. 1): S14–S19.
20. Gazzin S, Zelenka J, Zdrahalova L, Konickova R, Zabetta CC, Giraudi PJ, Berengeno AL, Raseni A, Robert MC, Vitek L, Tiribelli C. Bilirubin accumulation and *Cyp* mRNA expression in selected brain regions of jaundiced Gunn rat pups. *Pediatr Res.* 2012;7(6):653–660.
21. Schutta HS, Johnson L. Clinical signs and morphologic abnormalities in Gunn rat treated with sulfadimethoxine. *J Pediatr.* 1969;75(6):1070–1079.
22. Barker RA, Widner H. Immune problems in central nervous system cell therapy. *NeuroRx.* 2004;1(4):472–481.
23. Guillaume DJ, Johnson MA, Li XJ, Zhang SC. Human embryonic stem cell-derived neural precursors develop into neurons and integrate into the host brain. *J Neurosci Res.* 2006;84(6):1165–1176.
24. McBride JL, Behrstock SP, Chen EY, Jakel RJ, Siegel I, Svensen CN, Kordower JH. Human neural stem cell transplants improve motor function in a rat model of Huntington's disease. *J Comp Neurol.* 2004;475(2):211–219.
25. Hachiya Y, Hayashi M. Bilirubin encephalopathy: a study of neuronal subpopulations and neurodegenerative mechanisms in 12 autopsy cases. *Brain Dev.* 2008;30(4):269–278.
26. Hauser KF, Osborne JG, Stiene-Martin A, Melner MH. Cellular localization of proenkephalin mRNA and enkephalin peptide products in cultured astrocytes. *Brain Res.* 1990;522(2): 347–353.
27. Melner MH, Low KG, Allen RG, Nielsen CP, Young SL, Saneto RP. The regulation of proenkephalin expression in a distinct population of glial cells. *EMBO J.* 1990;9(3):791–796.

28. Björklund LM, Sanchez-Pernaute R, Chung S, Andersson T, IY, McNaught KS, Brownell AL, Jenkins BG, Wahlestedt C, Kim KS, Isacson O. Embryonic stem cells develop into functional dopaminergic neurons after transplantation in a Parkinson rat model. *Proc Natl Acad Sci.* 2002;99(4):2344–2349.
29. Fu MH, Li CL, Lin HL, Chen PC, Calkins MJ, Chang YF, Cheng PH, Yang SH. Stem cell transplantation therapy in Parkinson's disease. *SpringerPlus.* 2015;4:597.
30. Maucksch C, Vazey EM, Gordon RJ, Connon B. Stem cell-based therapy for Huntington's disease. *J Cell Biochem.* 2012; 114(4):754–763.
31. Tajiri N, Quach DM, Kaneko Y, Wu S, Lee D, Lam T, Hayama KL, Hazel TG, Johe K, Wu MC, Borlongan CV. Behavioral and histopathological assessment of adult ischemic rat brains after intracerebral transplantation of NSI-566RSC cell lines. *PLoS ONE* 2014;9(3):e91404.
32. Riess P, Zhang C, Saatman KE, Laurer HL, Longhi LG, Raghupathi R, Lenzlinger PM, Lifshitz J, Boockvar J, Neugebauer E, Snyder EY, McIntosh TK. Transplanted neural stem cells survive, differentiate, and improve neurological motor function after experimental traumatic brain injury. *Neurosurgery.* 2002;51(4):1043–1052, discussion 1052–4.